The surface is mildly curved at lower N_a but getting evener at higher N_a not only along the roadmap parameters but also with other parameters.

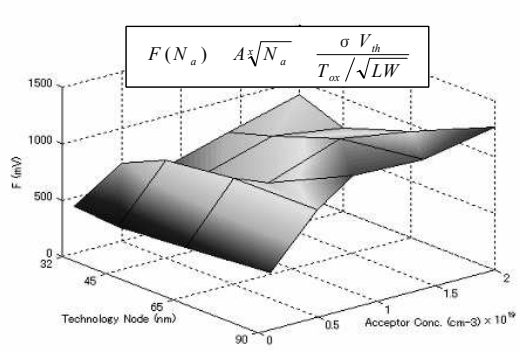

Fig. 3: Response surface of the concentration factor with various target parameters.

III. POWER SPECTRUM ANALYSIS

It is greatly helpful to characterize dopant distribution or potential field by the spatial frequency space because spatial frequency space is closely related with real space (Table 2). There is only 2D random noise observed for phase angle in spatial frequency space because discrete dopant is randomly and disorderly distributed. Its effect is considered to be the same level as baseline noise for all calculations. Therefore, only power is discussed in this work although phase angle is also important.

Table 2: Correspondence between real space and spatial frequency space.

Real Space	Spatial Frequency Space
Concentration Potential	Power Spectrum $P(u,v) = F_r(u,v)^2 + F_i(u,v)^2$
Position Interaction	Phase Angle $\xi = \tan^{-1}\frac{F_i(u,v)}{F_r(u,v)}$

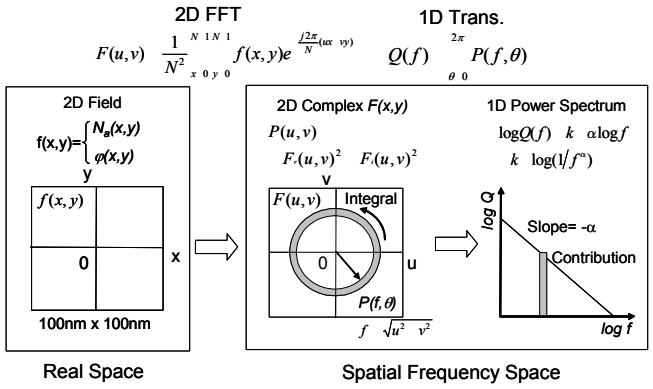

Fig. 4: Application of 2D FFT to f(x,y) and transformation to 1D power spectrum.

Fig. 4 shows the schematic procedure to apply FFT. F(u,v) is calculated by 2D FFT against 2D function f(x,y), which corresponds to concentration or potential field.

Power P(u,v) is defined as the square norm of the complex function of F(u,v), where $F_r(u,v)$ and $F_i(u,v)$ represent the real and imaginary part of F(u,v) respectively.

Because P(u,v) is a 2D function in spatial frequency space, it is still difficult to compare or characterize it directly. Therefore, P(u,v) is transformed to 1D power spectrum Q(f) by integrating P(f,θ) along all circumferences. 1D power Q(f) represents the contribution of each spatial frequency. Moreover, the slope characterizes the degree of the fluctuation.

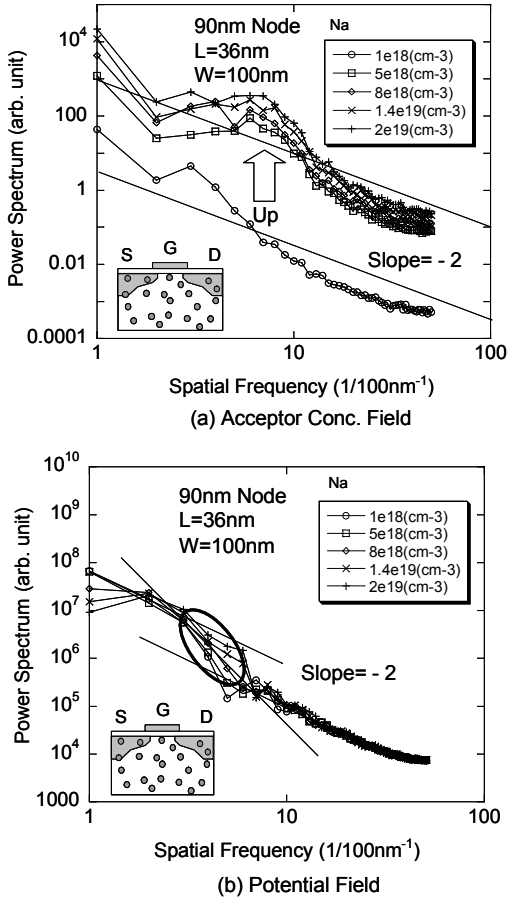

Fig. 5: 1D power spectrum for acceptor concentration field (a) and potential field (b) at the Si surface.

Fig. 5 (a) shows power spectrum for acceptor concentration field. Power is also observed to be saturated at higher acceptor concentration, which is similar in Fig. 2 and Fig. 3. Fig. 5 (b) shows the case of the potential field.

Both fields obey the $1/f^2$-rule generally because these fields are calculated from the second order of PDE for diffusion or potential. However, there is less noise in potential field than in concentration field. In potential field, high spatial frequency wave is eliminated from concentration field by solving the Poisson equation because the radius of the long-range part of Coulomb potential by an acceptor has

wider distribution than that of concentration, as is discussed later.

There is almost no concentration dependence among potential fields except for the specific frequency range of 5/100 nm^{-1} to 4/100 nm^{-1}. This spatial frequency range corresponds to the wave length of 20 nm to 25 nm.

IV. POTENTIAL FIELD WITH SPECIFIC WAVE LENGTH RANGE

There are two reasons why FFT is adopted to characterize fluctuation. One reason is to find what wave length range characterizes the fluctuation and the other reason is to reconstruct the original field with the specific wave length range by applying FFT using a window function.

Fig 6 (a) shows the original surface potential field with random dopant distribution. Fig. 6 (b) shows the reconstructed potential field by inverse FFT with waves above 20 nm wave length only.

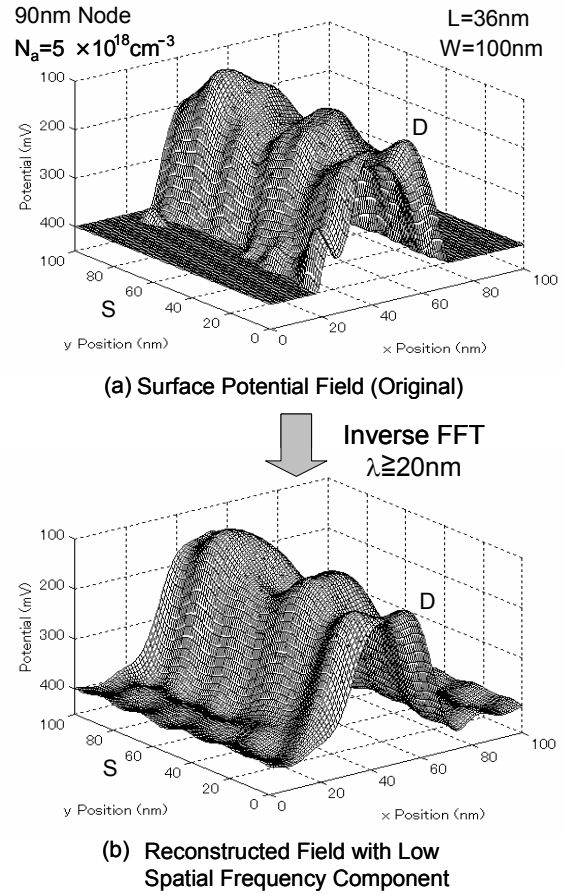

Fig. 6: Original surface potential field and reconstructed field by inverse FFT with waves above 20 nm wave length.

Comparing Fig. 6 (a) with Fig. 6 (b), the original potential field is almost reconstructed and the specific wave length takes a dominant role in fluctuation of Vth. Moreover, the Poisson equation behaves as a low-pass filter for concentration field because potential filed doesn't reflect the long-range part of individual impurities. Fig. 7 (a) shows relative acceptor concentrations for the long-range part of Sano model by an acceptor at the origin. Fig. 7 (b) shows the case of potential field. As N_a is increased, the relative acceptor concentration increases but the radius shrinks gradually. However, as for potential field, the peak value at the origin goes down but the radius stays almost constant in contrast to the concentration field.

Because potential field is described by overlapping these single waves, specific wave length is observed by Fourier analysis, whose range corresponds to the wave length of 20 nm to 25 nm.

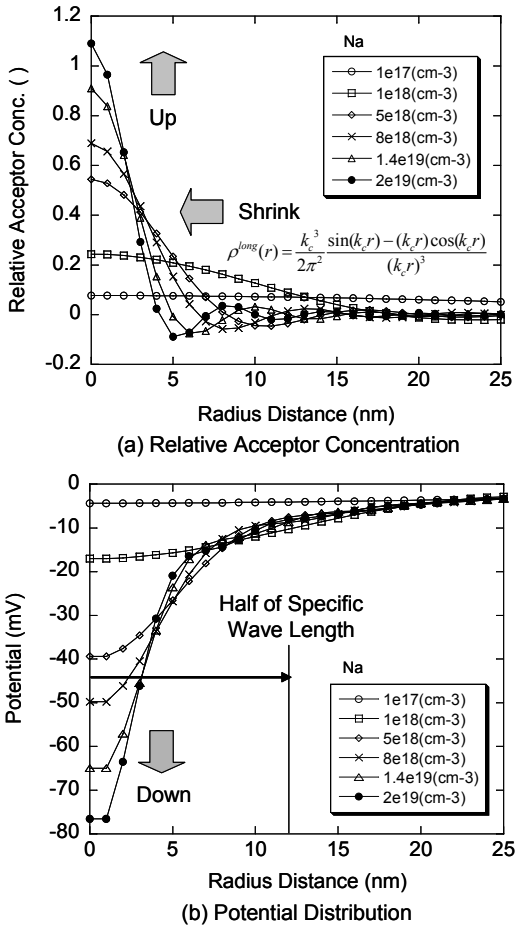

Fig. 7: Relative acceptor concentration (a) and its potential field (b) by an acceptor at the origin.

V. DISCUSSION

Assuming that the specific wave length in the potential field, there will be a new fluctuation caused by size effect between wave length and device size (Fig. 8).The potential field is fluctuated within a device for large scale devices. Scaling the device size, if N_a in the substrate is increased accordingly, potential is still averaged within a device (Center). But if the device size becomes smaller than specific wave length of 20 nm to 25 nm, the fluctuation is determined by the local potential field directly (Right). In such case, the frequency of Vth distribution will obey

Poisson distribution rather than symmetric normal distribution. Moreover, this will cause a fundamental problem to engineers in designing circuits with conventional 3σ criteria because Poisson distribution has broader distribution even if σ is the same level with that of normal distribution.

Geometry scaling is aggressive, while electrical properties, such as unit charge, dielectric, long-range part of Coulomb potential and so on, are kept almost constant. This unbalance for scaling causes the size effect.

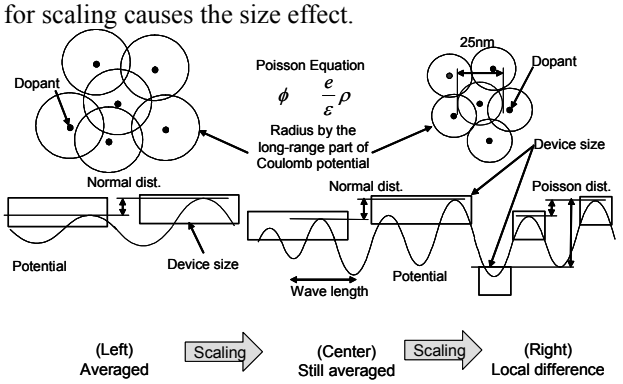

Fig. 8: Size effect by relative relation between device size and wave length of the potential fluctuation.

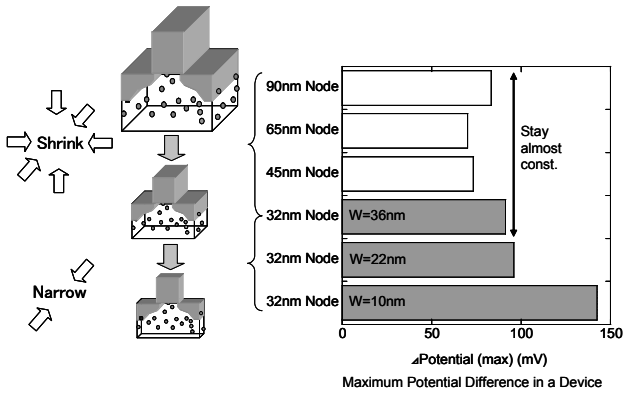

Fig. 9: Scaling rules and maximum potential difference in a device.

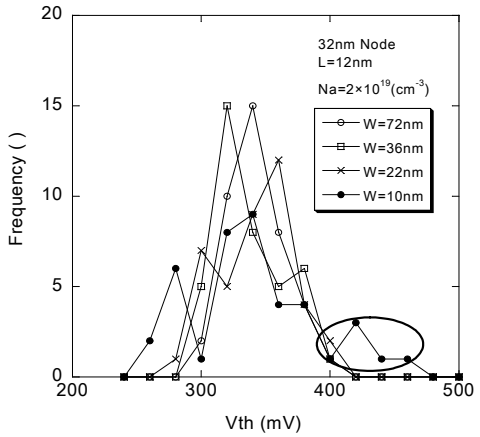

Fig. 10: Histogram of Vth Frequency distribution at 32 nm node with narrowing device.

Fig. 9 shows scaling rules to see the size effect and maximum potential difference in a device. There is a remarkable jump at 32 nm node with narrowing width.

Fig. 10 is the frequency of Vth distribution at 32 nm node for various device widths. Distribution is getting broader and lower with narrowing device.

Fig. 11 shows "normal probability plot", in which narrower width's curve deviates from others and it is the proof of departing from symmetric normal distribution. This means the increase of fluctuation should be notified because of the broader distribution tail due to Poisson distribution.

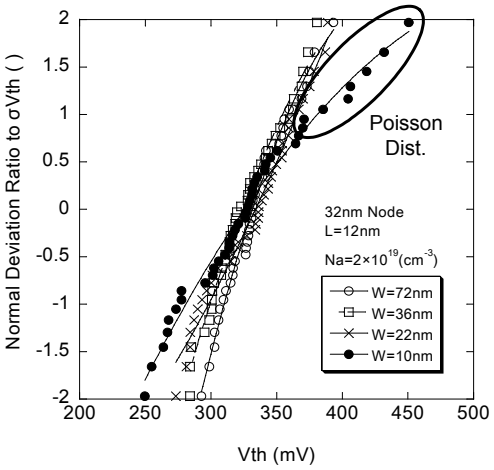

Fig. 11: Normal probability plot of σVth at 32 nm node with narrowing device.

VI. CONCLUSION

We have evaluated the device characteristics fluctuation against the technology roadmap. Absolute value of the fluctuation will be increased with scaling but concentration factor will be saturated for high acceptor concentration over 5 x 10^{18} cm^{-3}. Fourier analysis shows that power of spatial frequency generally obeys the $1/f^2$-rule and concentration dependence is less sensitive in potential filed than in concentration field.

This work suggests that it becomes hard to fabricate hundreds million transistors with uniform characteristics in a chip if device size is close to the specific wave length, 20 nm to 25nm, of the potential fluctuation especially.

REFERENCES

[1] Taurus-Process Reference Manual, Version W-2004.09, (Synopsys Inc., Mountain View, CA, 2004).

[2] Unpublished (http://www.selete.co.jp/).

[3] N. Sano *et al.*, IEDM Tech. Dig., pp. 275-278, 2000.

[4] T. Mizuno *et al.*, IEEE Trans. Electron Devices, vol. 41, pp. 2216-2221, 1994.

[5] A. Asenov *et al.*, IEEE Trans. Electron Devices, vol. 50, pp. 1837-1852, 2003.